Dual-band polarization beam splitter based on cascaded multimode anti-symmetric apodized Bragg gratings

Guanglian Cheng[1], Qiyuan Yi[1], Zengfan Shen[1], Zhiwei Yan[1], Qiyuan Li[1], Xinzhe Xiong[1], Fanglu Xu[1], Shuang Zheng[1], Shuai Cui[1], Yuan Yu[1], Yi Zou, Chaotan Sima[1] and Li Shen[1*]

[1]Wuhan National Laboratory for Optoelectronics and School of Optical and Electronic Information, Huazhong University of Science and Technology, Wuhan, China;

[2]The School of Information Science and Technology, ShanghaiTech University, Shanghai, China;

**Email: lishen@hust.edu.cn*

Abstract: We design and demonstrate a dual-band polarization beam splitter with insertion losses of 0.5/1.2dB and 3.1/1.1dB for TE/TM-polarizations at 1550 and 2000nm, respectively. The measured bandwidths for extinction ratio >20dB are ~115/100nm for 1.55/2µm waveband.

1. Introduction

Polarization beam splitters (PBSs) have been widely developed for on-chip polarization handling or polarization division multiplexing. Various on-chip PBSs have been developed based on different structures, including multimode interference (MMI) couplers [1], directional couplers (DCs) [2], Bragg grating [3], subwavelength gratings (SWGs) [4] and so on. Among these, PBSs based on Bragg grating or SWG structure exhibit large operation bandwidth (BW), exceeding 200nm for extinction ratio (ER) >20dB. It's worth noting that most of the reported PBSs are designed for the conventional O to L communication bands, which is currently the primary window for optical fiber communications. Recently, the 2µm waveband has emerged as a promising candidate for optical communication applications, thanks to the development of thulium-doped fiber amplifiers [5] and integrated light modulators [6]. To fully exploit the available spectral resources in both traditional communication and the 2µm waveband, integrated devices that are capable of dual-band operation are required [7,8].

In this paper, we propose and demonstrate a dual-band PBS that can be operated at both 1.55µm and 2µm wavebands, for the first time. We achieve the dual-band PBS function by cascading a dual-band TE_0/TE_1 mode (de)multiplexer and two multimode anti-symmetric apodized Bragg gratings (MASABGs) [9]. Theoretically, the designed device has insertion losses (ILs) as low as 0.1/0.4dB at 1550/2000nm. The theoretical operating BWs at 1.55µm and 2µm wavebands are up to 150nm and 180nm, respectively. The measured spectra of the fabricated device also exhibit wide BWs, and the BWs for ER >20 and >25dB are ~115nm and 105nm for the 1.55µm waveband, ~100nm and ~75nm for the 2µm waveband, respectively. In addition, the fabricated device shows ILs of 0.5/1.2dB at 1550nm and 3.1/1.1dB at 2000nm for TE/TM polarizations.

2. Design and simulation

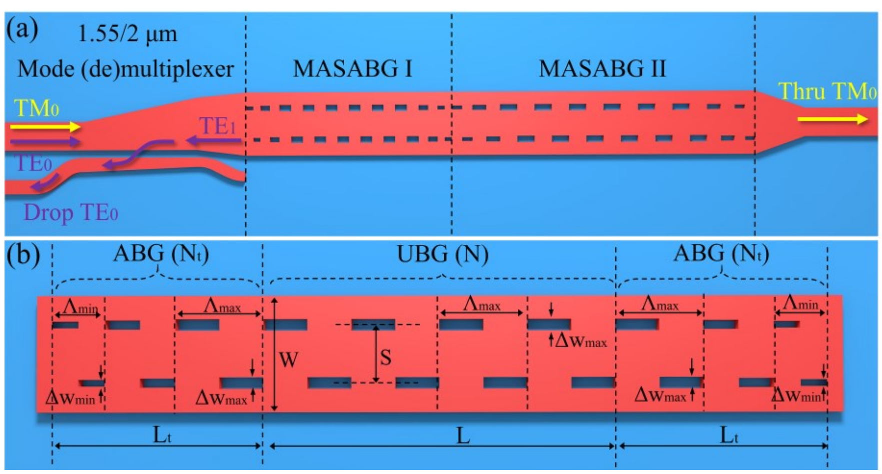

Fig. 1. (a) Schematic diagram of the proposed PBS with some key parameters labeled. The black dashed lines show the three parts of the device, i.e. a dual-band TE_0/TE_1 mode (de)multiplexer and two MASABGs. The yellow arrows show the propagation of the TE polarization, and the purple arrows represent the propagation of the TM polarization. (b) The proposed MASABG with some key parameters labeled. All the grating duty cycles are set to be 0.5. ABG: apodized Bragg grating, UBG: uniform Bragg grating.

Figure 1 (a) shows the schematic diagram of the proposed dual-band PBS. It is designed on the conventional 220-nm SOI platform with top silica cladding. The fabrication process for this device involves only one etching step. The whole device is composed of three parts, a dual-band TE_0/TE_1 mode (de)multiplexer, and two MASABGs. The dual-band TE_0/TE_1 mode (de)multiplexer is specifically designed to operate in both the 1.55μm and 2μm wavebands, whereas MASABG I and II are designed to convert the forward TE_0 mode into backward TE_1 mode for 1.55μm waveband and 2μm waveband, respectively. Here, the detailed parameters of MASABGs are marked in Fig. 1 (b). When 1.55μm or 2μm waveband TE_0 light is launched in the input port, the forward TE_0 mode is first converted into backward TE_1 mode through MASABG I or II, respectively. Subsequently, the reflected TE_1 mode is evolved into the TE_0 mode in waveguide B through the dual-band mode (de)multiplexer and finally output at the Drop-port. However, for the input TM polarization, phase matching conditions are not satisfied in both the 1.55μm and 2μm wavebands. Thus, the injected TM_0 mode will pass through the device with minimal loss and eventually output at the Thru-port. Consequently, this setup allows for the effective implementation of a dual-band PBS function.

To evaluate the performance of the proposed device, the 3D-FDTD method is used and the profiles of light propagation for TE_0/TM_0 modes at wavelengths of 1550nm and 2000nm are illustrated in Fig. 2 (a). It can be seen that when the 1.55μm waveband TE_0 mode is injected, it is first converted into the backward TE_1 mode by MASABG I, and then demultiplexed to the TE_0 mode at the Drop-port through the dual-band TE_0/TE_1 mode (de)multiplexer. For the 2μm waveband TE_0 mode, it first passes through the MASABG I with negligible loss. Subsequently, this forward TE_0 mode is converted into backward TE_1 mode through the MASABG II. Finally, the backward TE_1 mode is demultiplexed to the TE_0 mode through the dual-band TE_0/TE_1 mode (de)multiplexer and output at the Drop-port. On the other hand, the input TM_0 modes of the 1.55μm/2μm wavebands will pass through MASABG I and II and output at the Thru-port as the Bragg reflection condition doesn't satisfy. Figs. 2 (b)-(e) show the transmission spectrums calculated for the TE_0/TM_0 modes in the 1.55μm and 2μm wavebands. From these figures, the device exhibits excellent performance with ILs as low as 0.1dB and 0.4dB at around 1550nm and 2000nm, respectively. In addition, the calculated BWs for ER >20dB and >25dB are about 140nm and 130nm for the 1.55μm waveband, 150nm and 130nm for the 2μm waveband. It is worth noting that the operational BWs and ERs of our proposed device can be further improved by increasing the number and width of rectangular holes but will ultimately be limited by the operating BW of the dual-band TE_0/TE_1 mode (de)multiplexer.

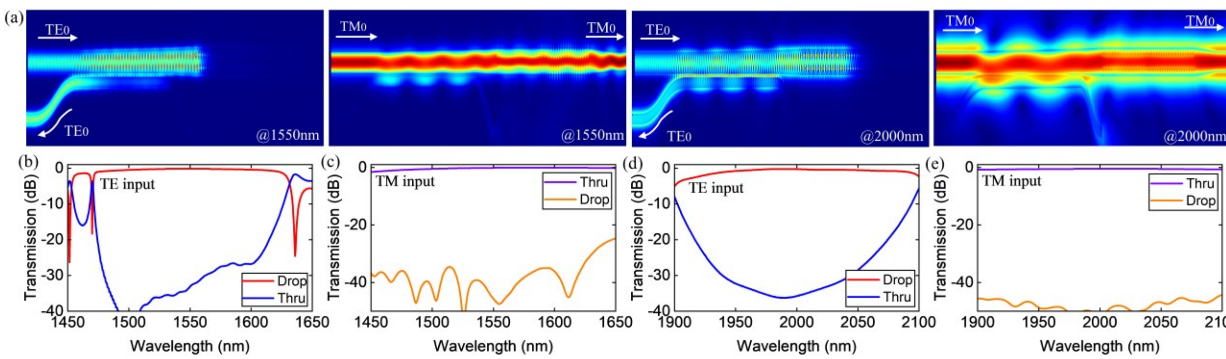

Fig. 2 (a) Light propagation profile for TE_0/TM_0 modes at wavelength of 1550/2000nm. Calculated transmission spectrums when (b) 1.55μm waveband TE_0 mode, (c) 1.55μm waveband TM_0 mode, (d) 2μm waveband TE_0 mode and (e) 2μm waveband TM_0 mode is launched.

3. Fabrication and results

The designed dual-band PBS is fabricated on an SOI wafer with a 220-nm thick top silicon layer and a 2μm thick buried dioxide layer. The device layout is patterned by 100 keV electron beam lithography (Vistec EBPG 5000plus ES). A single-step etching process is used to define all devices, followed by plasma-enhanced chemical vapor deposition (PECVD) of a 1μm thick top silica cladding for protection. Fully etched TE/TM-type GCs with center wavelengths of around 1550nm and 2000nm are also utilized to keep all devices at the same etch depth for easy fabrication. Since our proposed PBS can be operated at both the 1.55μm and 2μm wavebands, four set devices are fabricated with the same PBS but different GCs to characterize the performance. TE/TM-type GCs of 1.55/2μm wavebands are attached to both ends of the PBS to measure the transmission spectrums when TE/TM light is launched, as shown in Fig. 3 (a). Fig. 3 (b) shows the scanning electron microscope image for MASABG I and II. Figs. 3 (c) and (d) show the enlarged views of UBG in MASABG I and II, respectively. Straight single-mode waveguides are also fabricated on the same chip for normalization. The experimental setup consists of two laser sources: a 1.55μm waveband amplified spontaneous emission (ASE) source with a wavelength range covering from 1500nm to 1620nm and a home-built 2μm waveband ASE source with a wavelength range covering from 1960nm to 2060nm. The vertical coupling test system (OMTOOLS FA-H201M-N80) is used to input and output light to the device to be tested, where the input port is connected to the ASE light source and the output port is connected to the optical spectrum analyzer (OSA, Yokogawa AQ6375B). Figs. 3 (e) and (f) show the measured ILs and ERs of the fabricated PBS for TE and TM polarization at the 1.55μm waveband, whereas Figs. 3 (g) and (h) indicate the recorded ILs and ERs of the fabricated PBS for TE and TM polarization at the 2μm waveband. It can be seen that the ERs of TE and TM polarization at 1550nm and 2000nm are >30dB. For the 1.55μm waveband, the measured BWs for ER >20dB and >25dB are ~115nm and ~105nm, respectively, whereas the measured BWs for ER >20dB and >25dB are ~100nm and ~75nm, respectively, for the 2μm waveband. Moreover, the recorded ILs are 0.5/1.2dB at 1550nm and 3.1/1.1dB at 2000nm for TE/TM polarizations. The measured insertion losses are slightly higher than the simulated values, which can be attributed to waveguide sidewall roughness and fabrication errors.

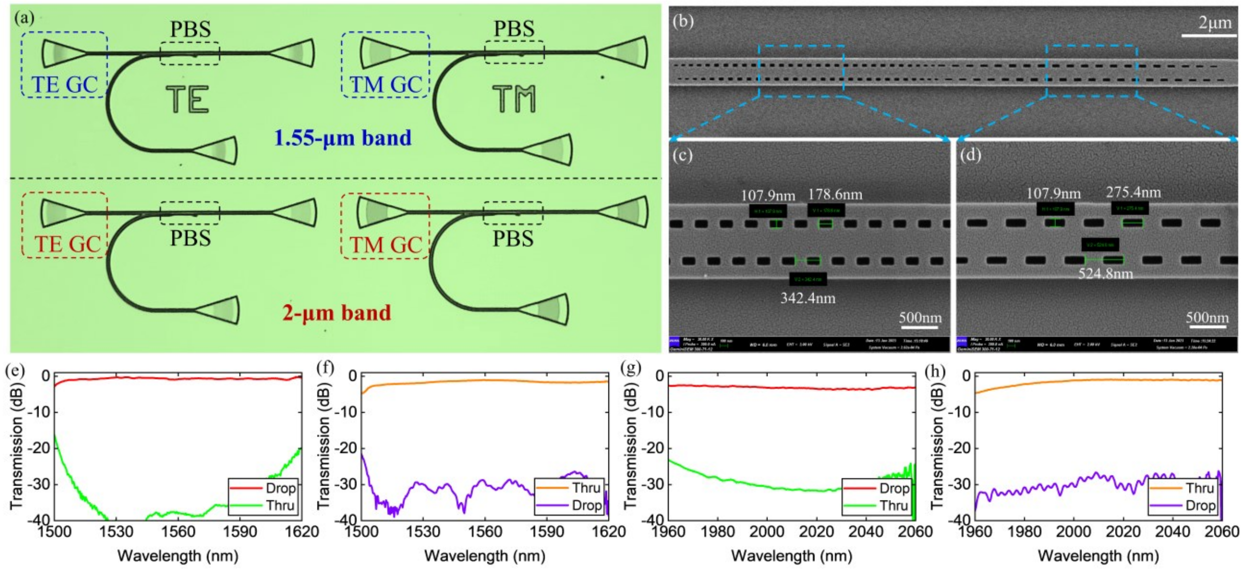

Fig. 3 (a) Microscopic image of fabricated four set devices for measurement. (b) Scanning electron microscope image for MASABG I and II. The enlarged views of UBG in MASABG (c) I and (d) II. Measured transmission spectrum for (e) 1.55μm waveband TE polarization, (f) 1.55μm waveband TM polarization, (g) 2μm waveband TE polarization and (h) 2μm waveband TM polarization.

4. Conclusion

In conclusion, we have designed and demonstrated a novel dual-band PBS capable of operating in both the 1.55μm and 2μm wavebands. The device is fabricated on the standard 220-nm SOI platform with a straightforward single-etch fabrication process. The designed device has a length of ~60μm. Simulated results show that the ILs are as low as 0.1dB and 0.4dB at around 1550nm and 2000nm, respectively, and the ERs are >20dB in a broadband wavelength range of 1475-1615nm and 1920-2070nm. For the fabricated dual-band PBS, the measured ILs are 0.5/1.2dB at 1550nm and 3.1/1.1dB at 2000nm for TE/TM polarizations, and the measured BWs for ER >20dB and >25dB are ~115nm and ~105nm for the 1.55μm waveband, ~100nm and 75nm for the 2μm waveband, respectively.

5. Acknowledgements

This work was supported in part by the National Key R&D Program of China (2022YFB2803600), in part by Natural Science Foundation of China (NSFC) (62175080).

6. References

[1] A. Herrero-Bermello, et al., "Experimental demonstration of metamaterial anisotropy engineering for broadband on-chip polarization beam splitting," Opt. Express, 28(11): 16385-16393 (2020).
[2] D. Dai, et al., "Ultrashort broadband polarization beam splitter based on an asymmetrical directional coupler," Opt. Lett., 36(13): 2590-2592 (2011).
[3] G. Cheng et al., "Silicon multimode anti-symmetric apodized Bragg gratings for ultra-broadband high-extinction-ratio polarization beam splitter," J. Lightwave Technol., in press (2023).
[4] H. Xu, et al., "Meta-Structured Silicon Nanophotonic Polarization Beam Splitter with an Optical Bandwidth of 415 nm," Laser Photon. Rev. 17, 2200550 (2023).
[5] Z. Li, et al., "Thulium-doped fiber amplifier for optical communications at 2 μm," Opt. Express, 21(8): 9289-9297 (2013).
[6] W. Cao, et al., "High-speed silicon modulators for the 2 μm wavelength band," Optica, 5(9): 1055-1062 (2018).
[7] Q. Yi, et al., "Silicon MMI-based power splitter for multi-band operation at the 1.55 and 2μm wave bands," Opt. Lett., 48(5): 1335-1338 (2023).
[8] M. Rouifed, et al., "Ultra-compact MMI-based beam splitter demultiplexer for the NIR/MIR wavelengths of 1.55 μm and 2 μm," Opt. Express, 25(10): 10893-10900 (2017).
[9] G. Cheng, et al., "Ultrahigh-extinction-ratio and broadband all-silicon TM-pass Polarizer by employing multimode anti-symmetric apodized Bragg grating," APL Photonics, 8: 046112 (2023).